CHAPTER VII
CREEP AND RECOVERY BEHAVIORS OF POLYTHIOPHENE-BASED ELECTRORHEOLOGICAL FLUID

7.1 Abstract

In this paper, we investigated the creep and recovery behaviors of PTAA particles in silicone oil suspensions upon the application of electric field. The effects of field strength, particle concentration, and the doping degree (conductivity values) on creep and recovery behaviors of the ER fluid were examined. The data show that the creep curves of this ER fluid consisted of both elastic and viscous responses at low stresses. With increasing stress, the fluid showed an instantaneous elastic response whereas the retarded elastic and the viscous responses diminished. After the removal of the applied stress, the strain decreased but did not completely relax to the original value indicating that this fluid exhibited a partially elastic recovery. The elastic recovery response decreased with increasing stress and then disappeared at some critical stress value, corresponding to the static yield stress. The equilibrium creep and recovery compliance parameters, J_C and J_R, were found to decrease with increasing particle concentration and particle conductivity. The recovery increased with increasing electric field strength, particle concentration, and particle conductivity. Moreover, the equilibrium compliance parameters at zero electric field, J_{Co} and J_{Ro}, strongly depend on the particle concentration and particle conductivity. The creep activation electric field, E_C, and the recovery activation electric field, E_R, depend only on the particle conductivity but they are independent of particle concentration.

KEYWORDS: Creep, Recovery, Polythiopnene, Electrorheological fluid

7.2 Introduction

Electrorheological (ER) fluids are typically composed of polarizable particles dispersed in a non-conducting fluid. Upon the application of an electric field, chain-like or fibrillar aggregates of the suspended particles are oriented along the direction of the electric field, thereby inducing viscoelasticity and a drastic increase in viscosity (Sakurai *et al.*, 1999). ER fluids have attracted considerable recently because their mechanical properties can be electrically controlled. Many applications based on ER technology have been developed, including the active elements of clutches, breaks, shock absorbers, engine mounts, valves, and flow pumps (Voyles *et al.*, 1996, Kamath and Wereley, 1997, Pfeiffer *et al.*, 1999). Many earlier studies have focused on investigating the yield stress and other rheological properties of ER fluids under steady shear and oscillatory shear flow (Li *et al.*, 2002). Nevertheless, ER fluids are typically operated under the conditions above the yield stress in various ER applications. The ER response under such conditions has been scarcely studied and it is not well understood. Creep and recovery testing may also be a good route to understand the rheological behavior of ER fluids. The creep is the time-dependent behavior of viscoelastic materials under a constant stress, whereby the sample is subjected to a constant shear stress while the strain is monitored as a function of time.

In this study, we hence investigated the ER behavior under creep testing of Poly (3-thiophene acetic acid), PTAA, doped with perchloric acid ($HClO_4$) in order to vary the conductivity of PTAA particles. The creep and recovery behaviors of PTAA suspensions were investigated under different constant stresses in electric field. The effects of stress level, electric field strength, and particle concentration were investigated and shall be reported here.

7.3 Experimental

7.3.1 Materials

3-thiopheneacetic acid, 3TAA (AR grade, Fluka) was used as the monomer. Anhydrous ferric chloride, $FeCl_3$ (AR grade, Riedel-de Haen) was used as the oxidant. Chloroform, $CHCl_3$ (AR grade, Lab-Scan) and methanol, CH_3OH (AR grade, Lab-Scan) were dried over CaH_2 for 24 hours under the nitrogen atmosphere and then distilled. The perchloric acid dopant, $HClO_4$ (AR grade, AnalaR) was used as received. The dispersing phase was silicone oil (AR grade, Dow corning) with density 0.96 g/cm^3 and kinematic viscosity of 100 cSt, and was vacuum-dried and stored in a desiccator prior to use.

7.3.2 Preparation of ER Fluid and Creep Measurements

Poly (3-thiopheneacetic acid), PTAA was synthesized by the oxidative-coupling polymerization according to the method of Kim *et al.* (Kim *et al.*, 1999). The PTAA particles were then doped with perchloric acid to control the particle conductivity (Chen *et al.*, 2000). The electrorheological, ER, fluids were prepared by dispersing $HClO_4$ doped PTAA particles in silicone oil (density 0.96 g/cm^3 and kinematic viscosity 100 cSt) with ultrasonicator for 30 minutes at 25 °C.

The creep and recovery behaviors were carried out using a stress-controlled rheometer (Carrimed, CR50) with 4 cm diameter parallel plate geometry at 25 ± 0.1 °C. The gap for the geometry used was 0.1 mm for each measurement. A DC voltage was applied during the measurements using a high voltage power supply (Bertan Associates Inc., Model 215). For initial conditioning, the suspensions were subjected to a steady shearing at 300 s^{-1} and then electrified in a quiescent state for 5 min to ensure the formation of equilibrium agglomerate structure before a measurement was taken. A constant stress was then instantaneously applied, maintained for 180 s, and suddenly removed. The time dependent of strain was measured at various electric field strengths. Each measurement was carried out at a temperature of 25 ± 0.1 °C and repeated at least two or three times.

7.4 Results and Discussion

Effects of stress level, particle concentration, and particle conductivity on the creep and recovery properties of the suspensions were investigated. Particle concentrations investigated were 5%, 10%, and 20% by weight (corresponding to volume fractions of 0.025, 0.048, and 0.092, respectively) at a specific conductivity of 7.5 x 10^{-2} S/cm (HPT5, HPT10, and HPT20). To study the effect of conductivity, the particle concentration was fixed at 20% by weight and the particle conductivity values investigated were approximately 3.2 x 10^{-7} (undoped, UPT20), 2.0x10^{-4} S/cm (low doping, LPT20), and 7.5 x 10^{-2} (high-doping, HPT20) S/cm, respectively.

In this section, a series of creep and recovery experiments were conducted with a sequence of step stresses. Creep is the time-dependent evolution in strain (γ) of a viscoelastic material under constant stress, σ_o, (Li et al., 2002). On the removal of stress, some of the time-dependent deformation is recoverable. A typical response to a creep test is characterized by two distinct phases: the creep phase and the recovery phase. In the creep phase, a constant stress (σ_o) is applied instantaneously to the sample and maintained at that level for a fixed period. For a viscoelastic material, the time dependence of creep strain (γ_C) can be expressed as follows;

$$\gamma_C(t) = \gamma_s + \gamma_d(t) + \gamma_v(t), \qquad (7.1)$$

where γ_s is the instantaneous strain which represents the elastic behavior, $\gamma_d(t)$ is a retardation strain which refer to as the delayed elastic strain which requires time for complete recovery, and $\gamma_v(t)$ is the viscous flow or the irreversible component of strain. For linear viscoelastic materials, the instantaneous strain γ_s is reversible and disappears on the removal of the applied stress. However, for nonlinear viscoelastic materials, the instantaneous strain γ_s may consist of an elastic component and a plastic component, γ_p; the latter cannot be recovered after unloading.

In the recovery phase in which the applied stress is suddenly removed, the instantaneous elastic response γ_s recovers immediately but the delayed elastic

response $\gamma_d(t)$ recovers gradually, while the viscous flow γ_v remains. Hence, the time dependent recovery strain $\gamma_R(t)$ is

$$\gamma_R(t) = \gamma_v + \gamma_d(t) \qquad (7.2)$$

On the other hand, the creep response might be expressed in the term of a parameter called the creep compliance J, in which $J(t) = \gamma(t)/\sigma_o$, because the stress remains constant. As indicated on Figure 7.1, the following parameters can be determined: the equilibrium creep compliance J_C and the equilibrium recovery compliance J_R (Ferry, 1980). J_C is the long-time behavior steady state compliance while J_R represents the steady state recovery compliance at long times after the stress is removed. If the sample has no internal structure, the creep may vary continuously with time, and the viscosity can be obtained from the inverse of the slope of the J(t) curve of the steady flow region (See *et al.*, 2004).

Figures 7.2 and 7.3 show the creep and recovery curves for a 20 wt % highly doped polythiophene suspension (HPT20) under a constant electric field strength of 1 kV/mm. We have recently reported that the yield stress value of the HPT20 suspension at field strength of 1 kV/mm is 76.5 Pa (Chotpattananont *et al.*, 2004). The creep tests were conducted below the yield stress regime: applied stresses were varied from 5 to 76.5 Pa.

From Figure 7.2, it appears that there is an initial jump in strain (the elastic response) and the strain curve in the creep phase comprises of three parts: the instantaneous strain, the retardation strain, and the viscous strain. Moreover, the sample shows an immediate strain recovery, followed by a slower recovery process when the applied stress is removed. At higher stress levels (10 Pa), the creep curve still contains the three strain components. The instantaneous strain on the removal of stress is smaller than that on the application of stress, i.e. $\gamma_s < \gamma_R(o)$, indicating that material becomes more plastic. We can expect that the degree of plasticity increases with the increase of the applied stress. This elastic-plastic behavior of the suspension may originate from the complex processes of rupture and reformation of the particle chains (Klingenberg *et al.*, 1990).

Figure 7.3 shows the creep and recovery curves for a 20 wt % suspension under the electric field strength of 1 kV/mm at applied shear stresses of 50, 70, 76.5 Pa. At the stresses of 50 and 70 Pa which are slightly below the yield stress of 76.5 Pa, the strains change abruptly and almost reach their equilibrium values instantaneously without the retarded strain or the viscous flow strain. It can be deduced from the curve that the suspension behaves nearly like an elastic solid. Furthermore, the strain recovery after the removal of stress is almost zero or no elastic strain occurs. The result suggests that when the applied stress is close to the yield stress, the plastic tendency becomes rather striking. As the applied shear stresses was increased to 76.5 Pa which is exactly at the yield stress level (Figure 7.3), we can see that the strain increases rapidly or elastically with time initially and then the strain keeps on increasing in a stepwise manner. Otsubo *et al.* suggested that at the critical stress $\tau_o = \tau_y$, the chain structure of ER fluid is subjected to both rupture and reformation processes (Ferry, 1980, Otsubo and Edamura, 1994). In addition, there was no instantaneous elastic recovery when the applied stress was removed. This indicates that the energy used for chain stretching at higher applied stress is not stored but is completely dissipated (Li *et al.*, 2002). Thus, the ER fluids show no elastic recovery after the removal of the critical stress or the yield stress.

The creep and recovery behaviors of the electrorheological and/or magnetorheological, MR, fluids have been reported in a few previously published papers. Otsubo and Edamura (Otsubo and Edamura, 1994) examined the creep and recovery properties of composite particles consisted of a polymer core and an inorganic shell dispersed in silicone oil. The core was 1,3-butyleneglycoldimethacrylate/butyl acrylate copolymer and the inorganic shells were a highly porous titanium dioxide. They reported that at low stresses this ER fluid behaved as a linear viscoelastic material. With increasing stress, the elastic and viscous strain responses decreased and the plastic contribution became more dominate. Similar to our results, the stepwise increasing in strain response was observed at the critical yield stress and no instantaneous elastic recovery took place when the applied stress was removed. The similar trend in creep and recovery responses was also observed in MR fluids. More recently, the commercially available hydrocarbon-based MR fluid (Li *et al.*, 2002) as well as the carbonyl iron

MR fluid (See *et al.*, 2004) have been investigated by Li et al. and See et al., respectively. They reported that the nonlinear viscoelastic, viscoplastic, or purely plastic properties of the MR fluid increased with increasing applied stress. When the strain was increased to the critical yield point, this MR fluid showed no elastic recovery after the removal of the critical stress. They suggested that the stored energy was completely consumed and the column structure changed to another metastable structure, thus the recovery disappeared.

Figure 7.4 shows the % recovery of the 20 % wt. HPT20 suspension as a function of applied stress at various electric field strengths. The recovery percentage was determined from the following equation (Cho *et al.*, 2004).

$$\% \text{ recovery} = \frac{(\gamma_i - \gamma_f)}{\gamma_i} \times 100 \qquad (7.3)$$

where γ_i is the total strain which is acquired before removing the applied stress, and γ_f is determined from the average value of strains when they have reached steady state values. The % recovery decreases with increasing applied stress and reaches zero value at around the yield point. Apparently, the suspension shows no recovery above the yield point. The recovery after the removal of stresses diminishes as the applied stress is increased. As noted by Li et al. (Li *et al.*, 2002), when the stress is increased upto the critical yield stress value, the stored energy is completely consumed and the particle chain structure changes an equilibrium configuration to another metastable configuration. Thus, the ER fluids show no elastic recovery at or above the critical stress (Li *et al.*, 2002).

Figure 7.5 shows the compliance response of the 20 %wt HPT20 suspension at a constant stress of 50 Pa subjected to various electric field strengths of 1, 2, and 3 kV/mm. In the creep phase, a decrease in the instantaneous creep compliance can be clearly observed with the increment of electric field strength. This result implies that the elastic component of this suspension decreases with increasing electric field strength. After the removal of the applied stress, the suspension shows some recovery process. However, the recovery compliance increases with the increasing

electric field strength, i.e. the suspension exhibits a greater recovery as the field strength is increased.

Furthermore, the equilibrium creep compliance J_C and the equilibrium recovery compliance J_R were then determined from the linear-linear plot of compliance and time as illustrated in Figure 7.2. The electric field dependent J_C and J_R parameters are shown in Figure 7.6 and Figure 7.7, respectively. It can be clearly seen that the J_C parameter significantly decreases as the electric field strength is increased while the J_R parameter increases. The decrease in J_C with increasing electric field strength is consistent with the generally accepted mechanism for the ER effect in particulate dispersions. On application of the field, the particles become polarized creating induced dipole moments, leading to interparticle attractions which result in the formation of fibrillar agglomerates in the suspension (Lee *et al.*, 2001). Higher field strength induces a higher dipole moment and increases the strength of the interparticle interactions creating longer agglomerates (Parthasarathy et al., 1994). These longer and stronger agglomerates result in higher rigidity, stiffer, and provide a greater resistance to the shear. From the Figure 7.6 and Figure 7.7, it is obvious that the J_C and J_R parameters decrease with particle concentration at any specified electric field strength, i.e. the values of J_C and J_R increase in the order HPT20 < HPT10 < HPT5.

From Figure 7.6, we may deduce that the electric field dependence of J_C parameter can be written as

$$J_C = J_{Co}e^{-E/E_C} \qquad (7.4)$$

where J_{Co} is the creep compliance at zero electric field, and E_C is the creep *activation* electric field. The values of J_{Co} and E_C deduced from the fits in Figure 7.6 are tabulated in Table 7.2. In the recovery phase, the electric field dependence of J_R parameter can also be fitted by the relationship of

$$J_R = J_{Ro}e^{E/E_R}, \qquad (7.5)$$

where J_{Ro} is the recovery compliance at zero field, and E_R is the recovery *activation* electric field. From Figure 7.7, the values of J_{Ro} and E_R for the HPT5, HPT10, and HPT20 suspensions were determined and are tabulated in Table 7.2.

Figure 7.8 shows the % recovery of polythiophene suspensions as a function of the electric field strength at various particle concentrations. As the electric field strength increases, the recovery percentage increases at a fixed applied stress. This implies that the suspension becomes more solidified as the electric field strength increases. Moreover, the % recovery also increases with increasing particle concentration. This might be due to the fact that an increase of concentration typically results in increases in density and the thickness of fibrillar agglomerates. These larger agglomerates provide a superior resistance to the shear flow.

Figure 7.9 and Figure 7.10 show the effect of particle conductivity on the values of J_C and J_R of 20 wt % $HClO_4$ doped polythiophene suspensions at various electric field strengths. At a specific electric field strength, the J_C and J_R parameters decrease with particle conductivity, i.e. the values of J_C and J_R increase in the order HPT20 < LPT20 < UPT20. The J_C and J_R parameters also exhibit the electric field dependence of the forms $J_C = J_{Co}e^{-E/E_C}$ and $J_R = J_{Ro}e^{E/E_R}$, respectively. The values of J_{Co} and E_C deduced from the fits in the creep phase (Figure 7.9) and the values of J_{Ro} and E_R in the recovery phase (Figure 7.10) are tabulated in Table 7.2.

From Table 7.2, it can be clearly seen that the compliance parameters at zero electric field, J_{Co} and J_{Ro}, strongly depend on the particle concentration and particle conductivity. The values of J_{Co} and J_{Ro} decrease with increasing particle concentration and particle conductivity. The particle conductivity dependence may possibly arises from electrostatic interactions between particles. Moreover, it can be deduced from Table 7.2 that the creep *activation* electric field, E_C, in the creep phase depends on the particle conductivity but it is independent of particle concentration. The similar trend can be observed also in the recovery phase in which the recovery electric field, E_R, exhibits particle concentration independence but it depends on particle conductivity. The particle conductivity dependences of E_C and E_R can be apparently observed at high doping levels; the E_C and E_R values of the HPT20 suspension are higher than those of LPT20 and UPT20. It might due to the fact that the behavior of ER fluids can be generally described using the electrostatic

polarization model (Klingenberg *et al.*, 1991), which arises due to the mismatch between the complex components of the dielectric permittivity of the particles and the medium. The net force on each sphere is the sum of its interactions with all other spheres. The interaction between particles is predicted to be proportional to the square of the electric field, E^2, particle concentration, and particle conductivity as $F \propto \phi K_f E^2 \beta^2$, where ϕ is the volume fraction of particles, K_f is the dielectric permittivity of the continuous medium, and β is the relative polarizability, which under DC or low frequency AC fields, is controlled by the conductivities of the particles and continuous medium (Parthasarathy and Klingenberg, 1996). The increase of particle concentration and particle conductivity results in stronger interparticle interactions, higher rigidity, stiffer, and provide a greater resistance to the shear as indicated by a lower shear strain or the creep and recovery compliance parameters.

Figure 7.11 shows the effect of particle conductivity on the % recovery of polythiophene suspensions. The %recovery also increases with increasing of electric field strength and particle conductivity.

7.5 Conclusions

In this study, the creep and recovery behaviors of poly(3-thiopheneacetic acid) suspension has been investigated. Our results indicate that our ER suspensions behave like a viscoelastic solid under the electric field with a combination of elasticity, plasticity, and viscosity behaviors. With increasing stress, the fluids show instantaneous elastic response whereas the retarded elastic and the viscous responses decrease. After the removal of the applied stress, the strain decreases but does not completely relax to its original value which indicates that this fluid exhibits a partially elastic recovery. The elastic recovery response decreases with increasing stress and then disappears at some critical stress value, corresponding to the static yield stress. When the stress is increased above the yield stress, the fluid exhibits a purely liquid response in which the strain continuously increases with time. Moreover, the equilibrium compliance parameters, J_C and J_R, were found to decrease

with increasing particle concentration and particle conductivity. In both creep and recovery phases, the equilibrium compliance parameters at zero electric field, J_{Co} and J_{Ro}, strongly depend on the particle concentration and particle conductivity. The values of J_{Co} and J_{Ro} decrease with increasing particle concentration and particle conductivity. The creep *activation* electric field, E_C, and the recovery *activation* electric field, E_R, depend only on the particle conductivity but are independent of particle concentration. In addition, the recovery increases with the increasing of the electric field strength, particle concentration, and particle conductivity.

7.6 Acknowledgements

The authors are grateful for the financial supports provided by The Thailand Research Fund (TRF): TRF-RGJ grant no. PHD/0128/2542; and TRF-BGJ grant no. BGJ/03/2544, the Petroleum and Petrochemical Consortium, and the Electroactive and Conductive Polymers Research Unit.

7.7 References

Sakurai, R., See, H., Saito, T., Asai, S., and Sumita, M. (1999). Suspension of layered particles: an optimum electrorheological fluid for d.c. applications. Rheol. Acta, 38(5), 478-483.

Voyles, R.M., Fedder, G., and Khosla, P.K. (1996). Design of a modular tactic sensor and actuator based on an electrorheological gel. Proceeding of the 1996 IEEE International Conference on Robotics and Automation, 13-17.

Kamath, G.M. and Wereley, N. (1997). A nonlinear viscoelastic-plastic model for electrorheological fluids. Smart Mater. Struct., 6, 351-359.

Pfeiffer, C., Mavroidis, C., Celestino, C., and Cohen, Y.B. (2000). Controlled compliance haptic interface using electro-rheological fluids. Proceedings of the SPIE Smart Structures Conference, 3987, 1-11.

Li, W.H., Du, H., Chen, G., and Yeo, S.H. (2002). Mater. Sci. Eng. A., 333, 368.

Kim, B., Chen, L., Gong, J., and Osada, Y. (1999). Titration behavior and spectral transitions of water-soluble polythiophene carboxylic acids. Macromolecules, 32(12), 3964-3969.

Chen, L., Kim, B., Nishino, M., Gong, J., and Osada, Y. (2000). Environmental responses of polythiophene hydrogels. Macromolecules, 33(4), 1232-1236.

See, H., Chen, R., and Keentok, M. (2004). Colloid Polym. Sci., 282, 423.

Klingenberg, D.J. and Zukoski, C.F. (1990). Studies on the steady-shear behavior of electrorheological suspensions. Langmuir, 6(1), 15-24.

Cho, M.S., Lee, J.H., and Choi, H.J. (2004). J. Maters. Sci., 39, 1377.

Lee, Y.H., Kim, C.A., Jang, W.H., Choi, H.J., and Jhon, M.S. (2001). Synthesis and electrorheological characteristics of microencapsulated polyaniline particles with melamine–formaldehyde resins. Polymer, 42(19), 8277-8283.

Parthasarathy, M., Ahn, K.H., Belongia, B.M., and Klingenberg, D.J. (1994). The role of suspension structure in the dynamic response of electrorheological suspensions. Inter. J. Mod. Phys. B, 8(20&21), 2789-2809.

Klingenberg, D.J., Swol, F.V., and Zukoshi, C.F. (1996). The small shear rate response of electrorheological suspensions: I. Simulation in the point-dipole limit. J. Chem. Phys., 94(9), 6160-6168.

Klingenberg, D.J., Swol, F.V., and Zukoshi, C.F. (1996). The small shear rate response of electrorheological suspensions: II. Extension beyond the point-dipole limit. J. Chem. Phys., 94(9), 6170-6178.

Chotpattananont, D., Sirivat, A., and Jamieson, A.M. (2004). Scaling of yield stress of polythiophene suspensions under electric field. Macromolecular Mats. & Eng., 289, 434.

Otsubo, Y. and Edamura, K. (1994). J. Rheol., 38, 1721.

Table 7.1 Properties and yield stress values of PTAA/silicone oil suspensions

ERFs	Particle Concentration (%wt.)	Particle Conductivity (S/cm)	Yield Stress, σ_y (Pa)				
			1 kV/mm	1.5 kV/mm	2 kV/mm	2.5 kV/mm	3 kV/mm
HPT5	5	7.5×10^{-2}	20.1	38.5	60.1	113.8	126.5
HPT10	10	7.5×10^{-2}	43.5	84.4	146.1	184.8	275.8
HPT20	20	7.5×10^{-2}	76.5	115.0	187.3	250.3	340.6
LPT20	20	2.0×10^{-4}	44.3	95.5	167.8	221.0	308.1
UPT20	20	3.2×10^{-7}	38.5	58.5	96.5	200.25	286.0

Table 7.2 Values of the equilibrium compliance parameters and the activation electric field of PTAA/silicone oil suspensions

ERFs	Creep Phase		Recovery Phase	
	J_{Co} (1/Pa)	E_C (kV/mm)	J_{Ro} (1/Pa)	E_R (kV/mm)
HPT5	-2.46	2.87	-5.14	2.35
HPT10	-2.87	2.64	-5.48	2.41
HPT20	-3.36	2.56	-5.73	2.60
LPT20	-3.22	4.06	-5.83	1.86
UPT20	-2.63	3.95	-5.54	1.74

* The parameters are determined from equations of $J_C = J_{Co}\, e^{-E/E_C}$ and $J_R = J_{Ro}\, e^{-E/E_R}$.

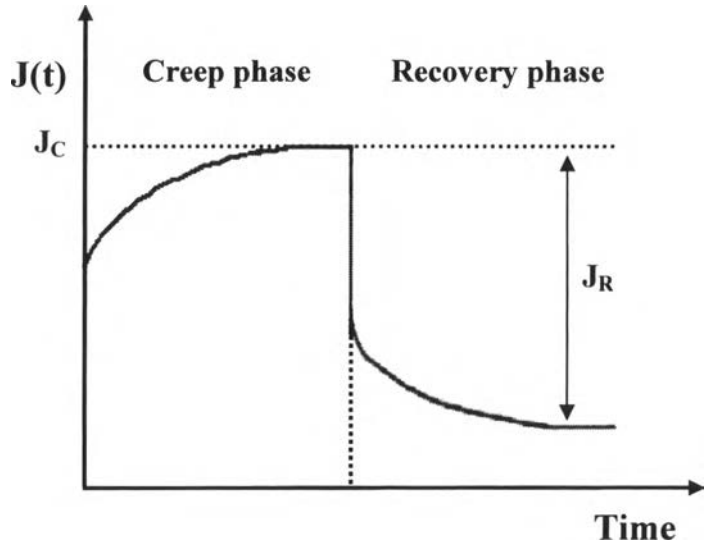

Figure 7.1 Schematic diagram of the creep curve under a constant applied shear stress and the recovery curve in the absence of the applied stress for a typical viscoelastic material.

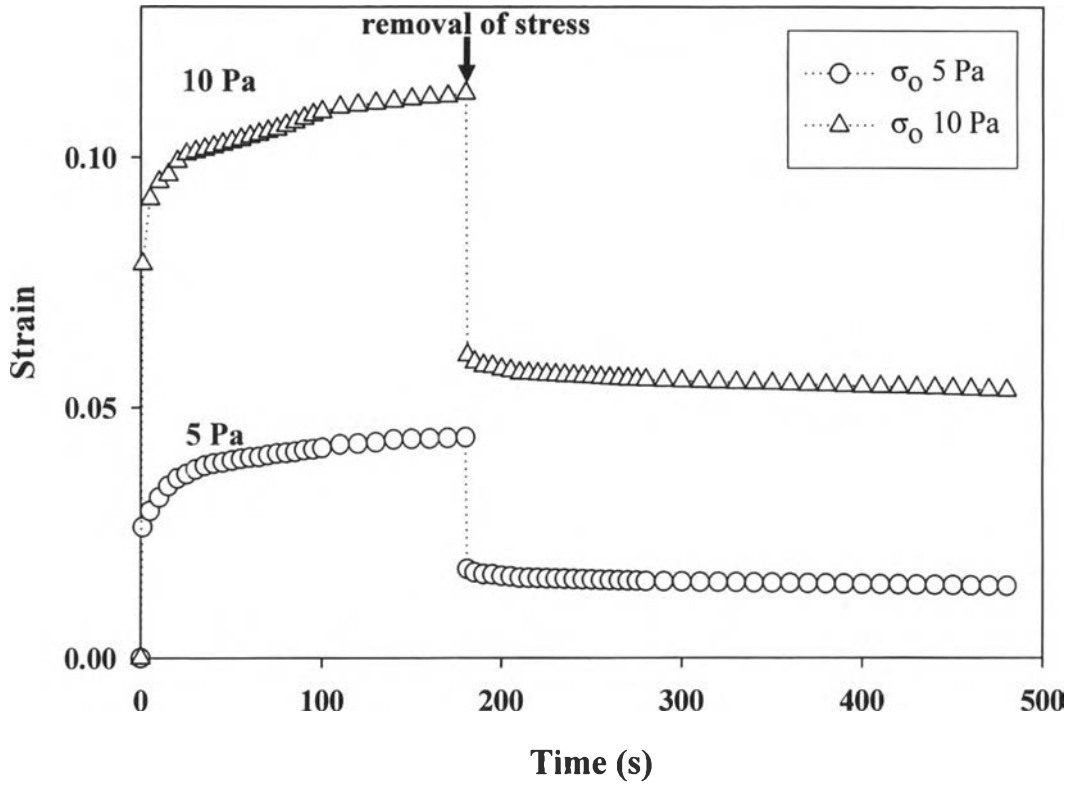

Figure 7.2 Creep and recovery curves of the 20 wt% highly doped PTAA suspension under the electric field strength of 1 kV/mm at various applied stress values: (O) 5 Pa and (Δ) 10 Pa.

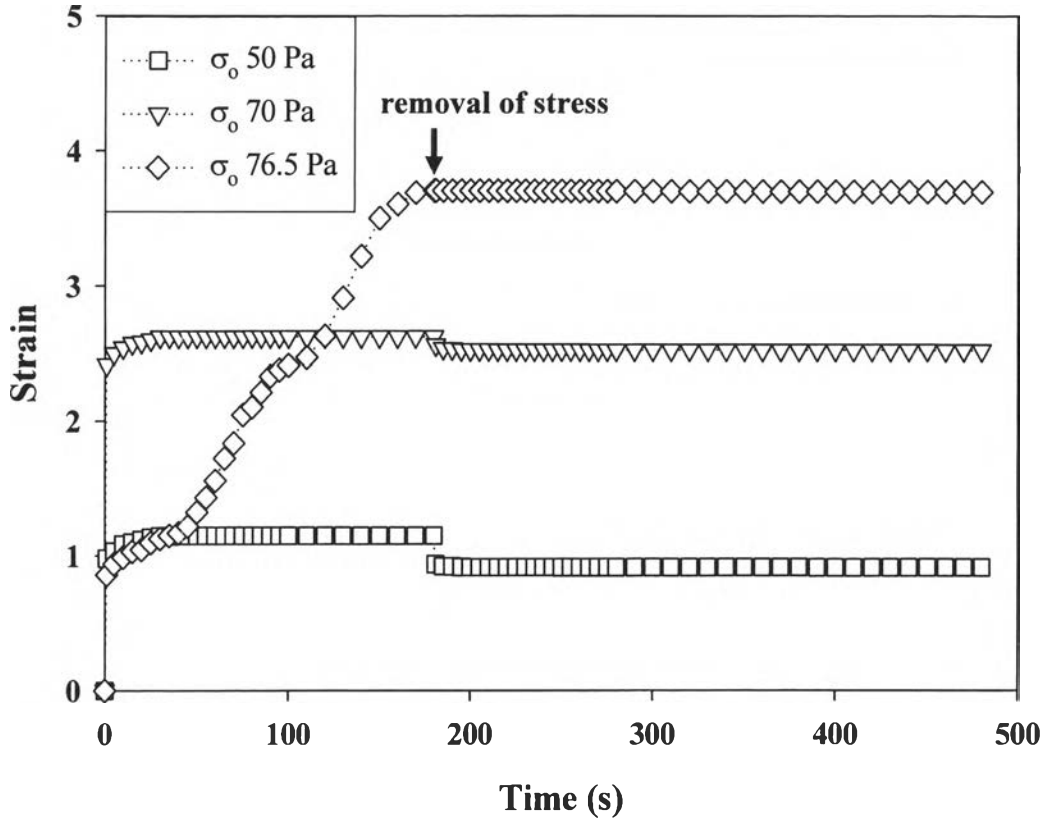

Figure 7.3 Creep and recovery curves of the 20 wt% highly doped PTAA suspension under the electric field strength of 1 kV/mm at various applied stress values: (□) 50 Pa, (▽) 70 Pa, and (◊) 76.5 Pa.

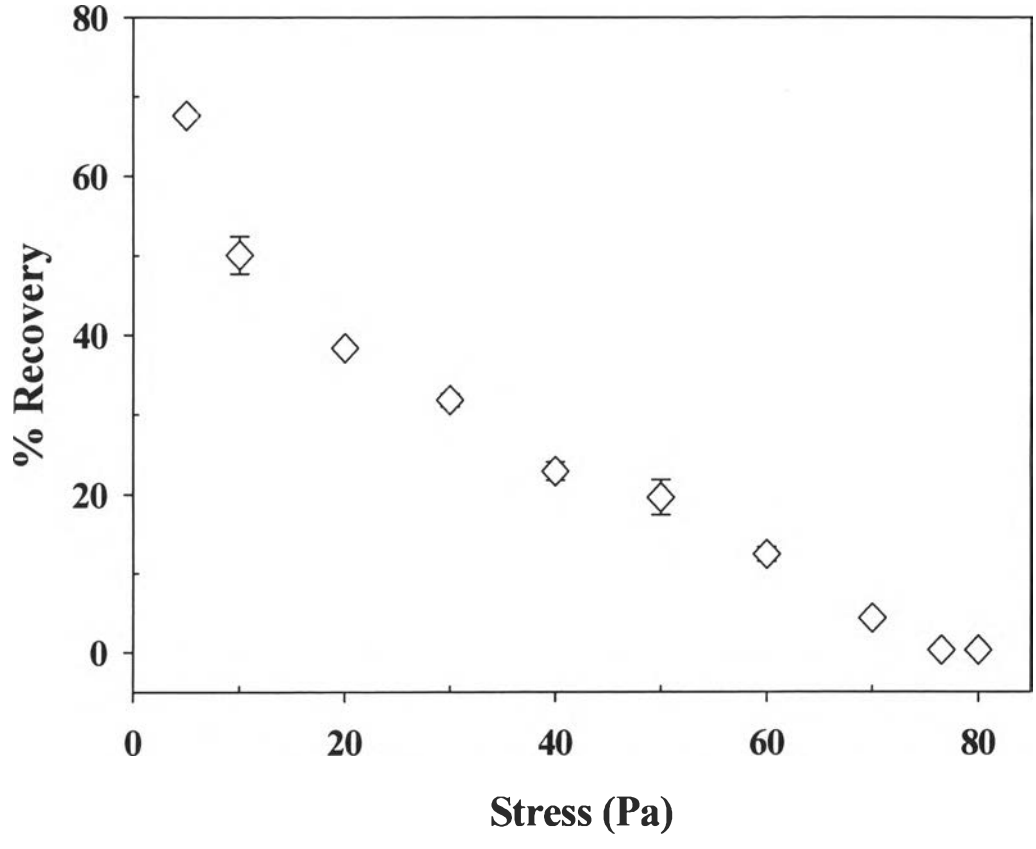

Figure 7.4 The % recovery as a function of the applied stress of 20% wt highly doped PTAA suspension under electric field strength of 1 kV/mm.

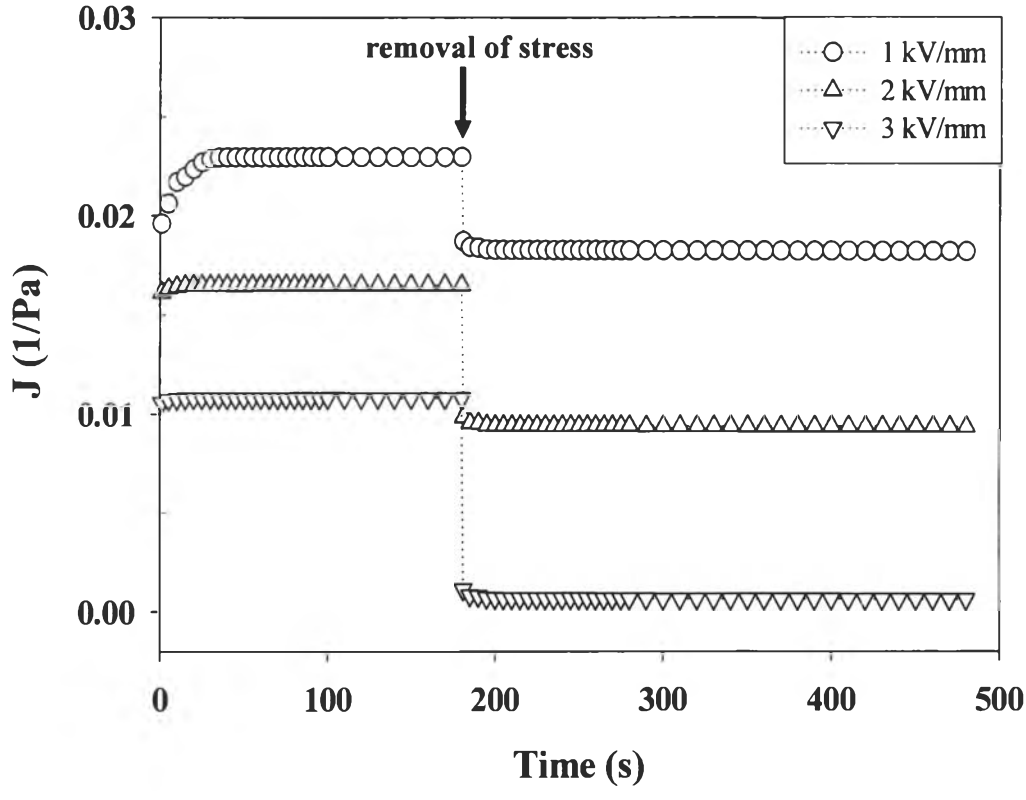

Figure 7.5 Creep and recovery curves of the 20 wt% highly doped PTAA suspension at a constant applied stress value of 50 Pa at various electric field strengths.

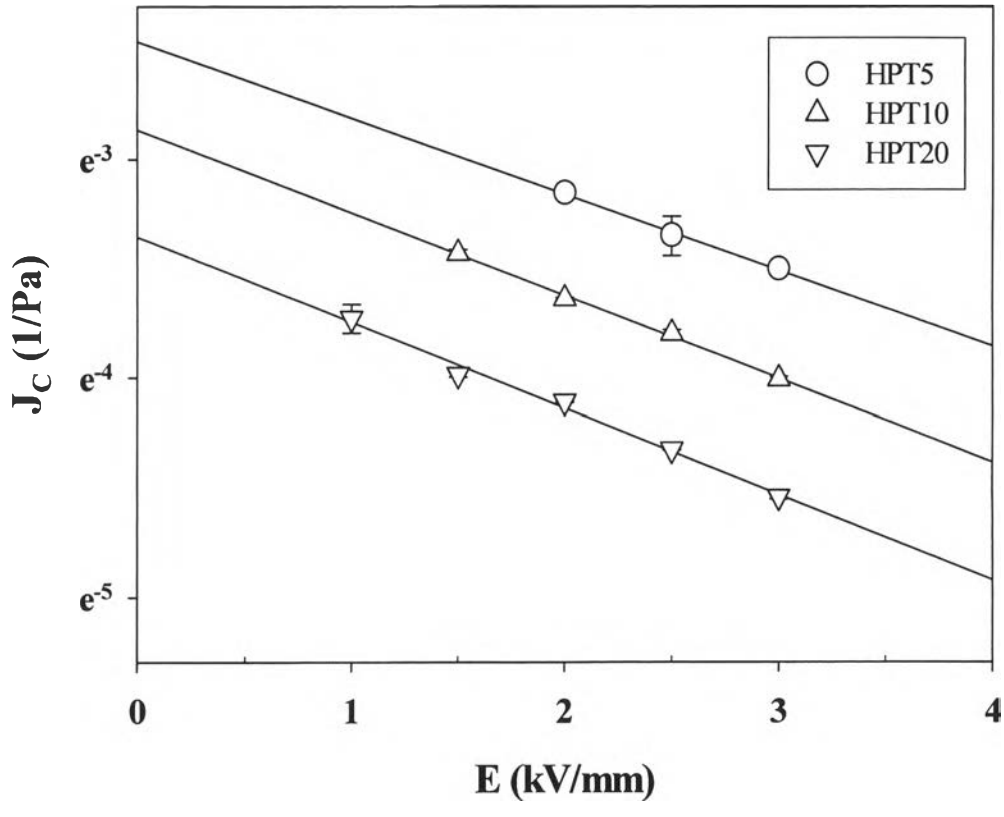

Figure 7.6 Equilibrium creep compliance, J_C, of highly doped PTAA suspensions at a constant applied stress of 50 Pa at various electric field strengths.

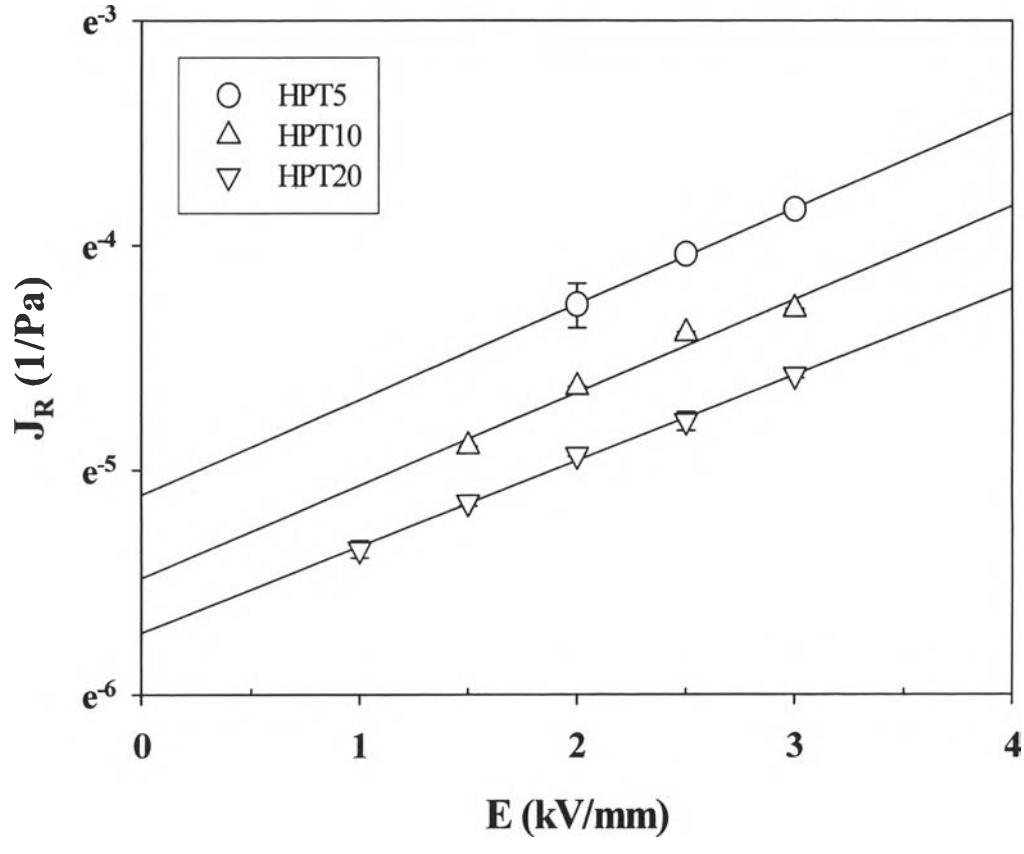

Figure 7.7 Equilibrium recovery compliance, J_R, of the highly doped PTAA suspensions at a constant applied stress of 50 Pa at various electric field strengths.

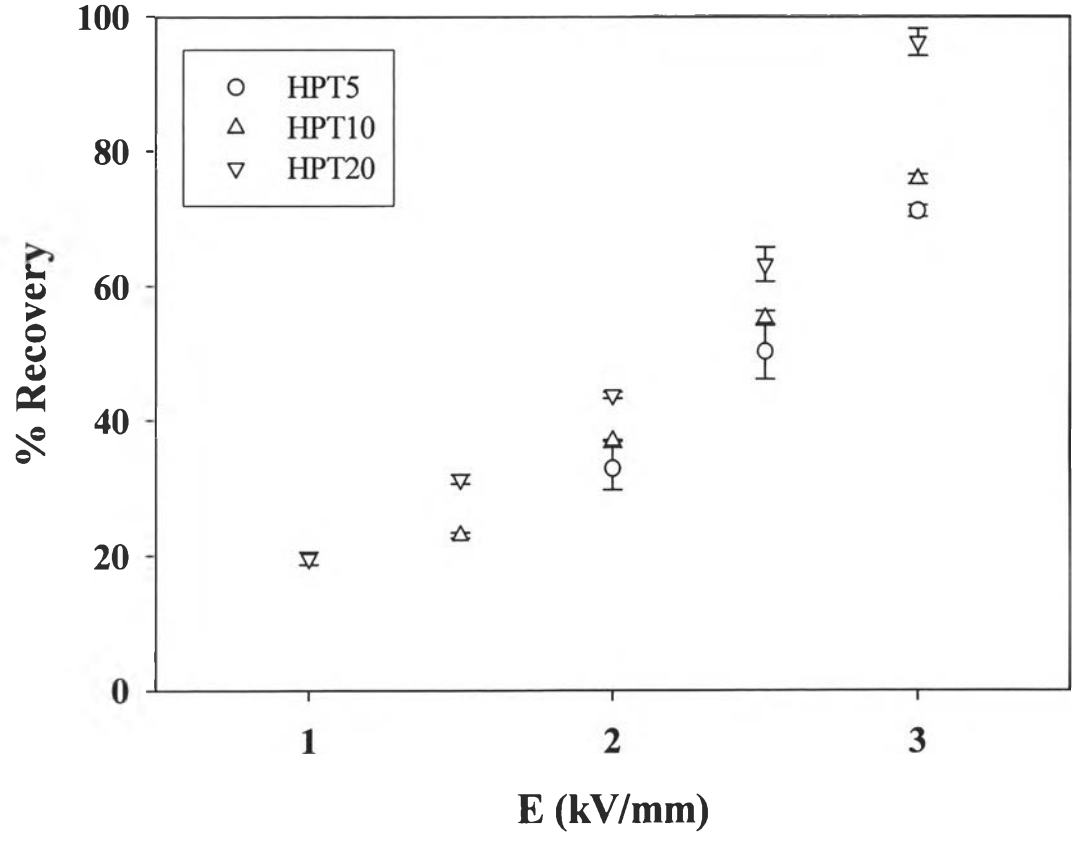

Figure 7.8 The % recovery as a function of the electric field strength of highly doped PTAA suspensions at a constant applied shear stress of 50 Pa.

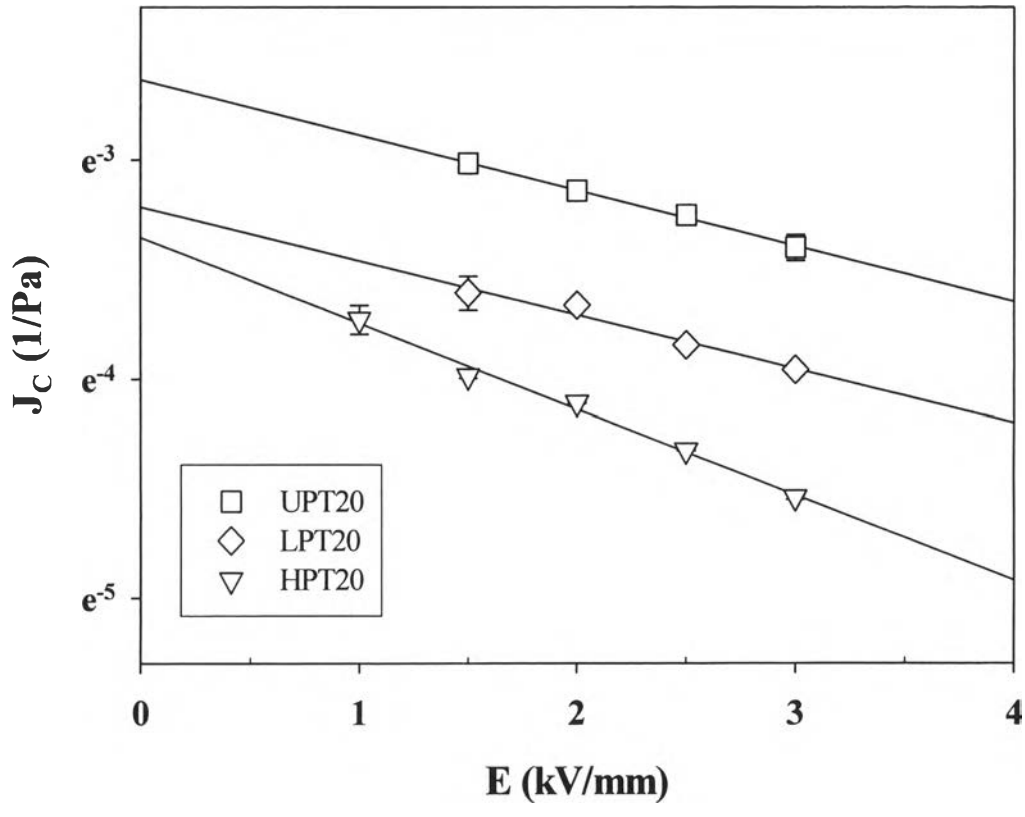

Figure 7.9 Equilibrium creep compliance, J_C, of 20% wt doped PTAA suspensions at a constant applied stress of 50 Pa at various electric field strengths.

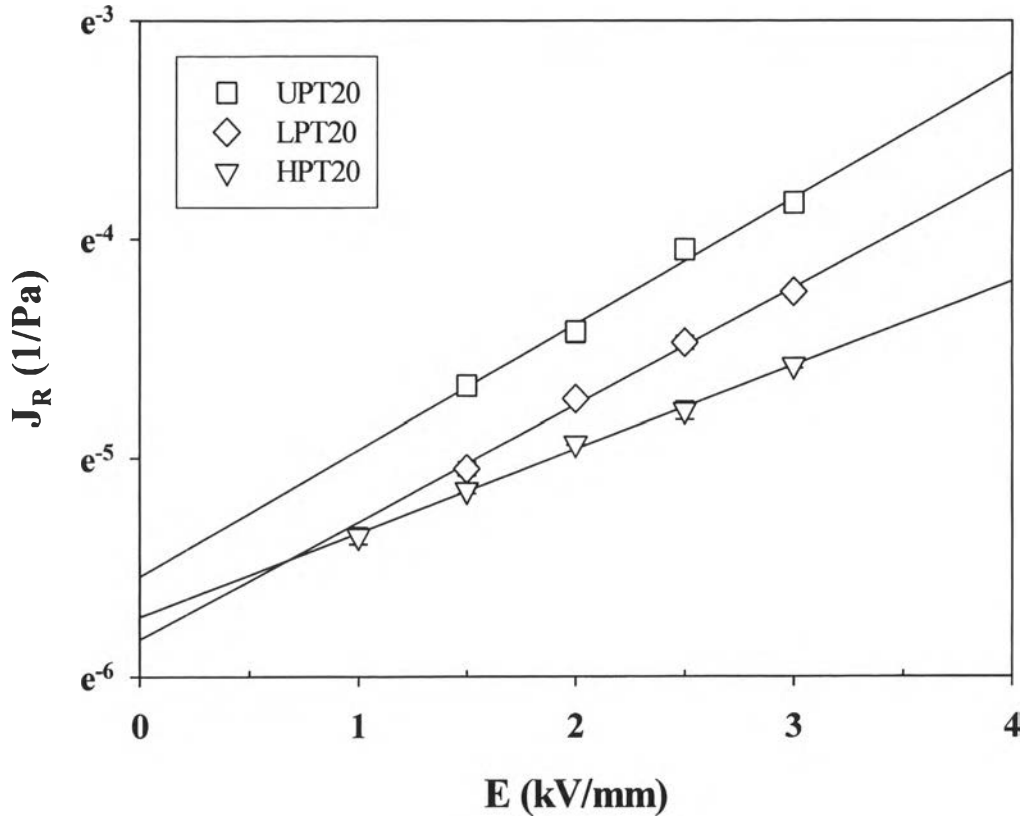

Figure 7.10 Equilibrium recovery compliance, J_R, of 20% wt doped PTAA suspensions at a constant applied stress of 50 Pa at various electric field strengths.

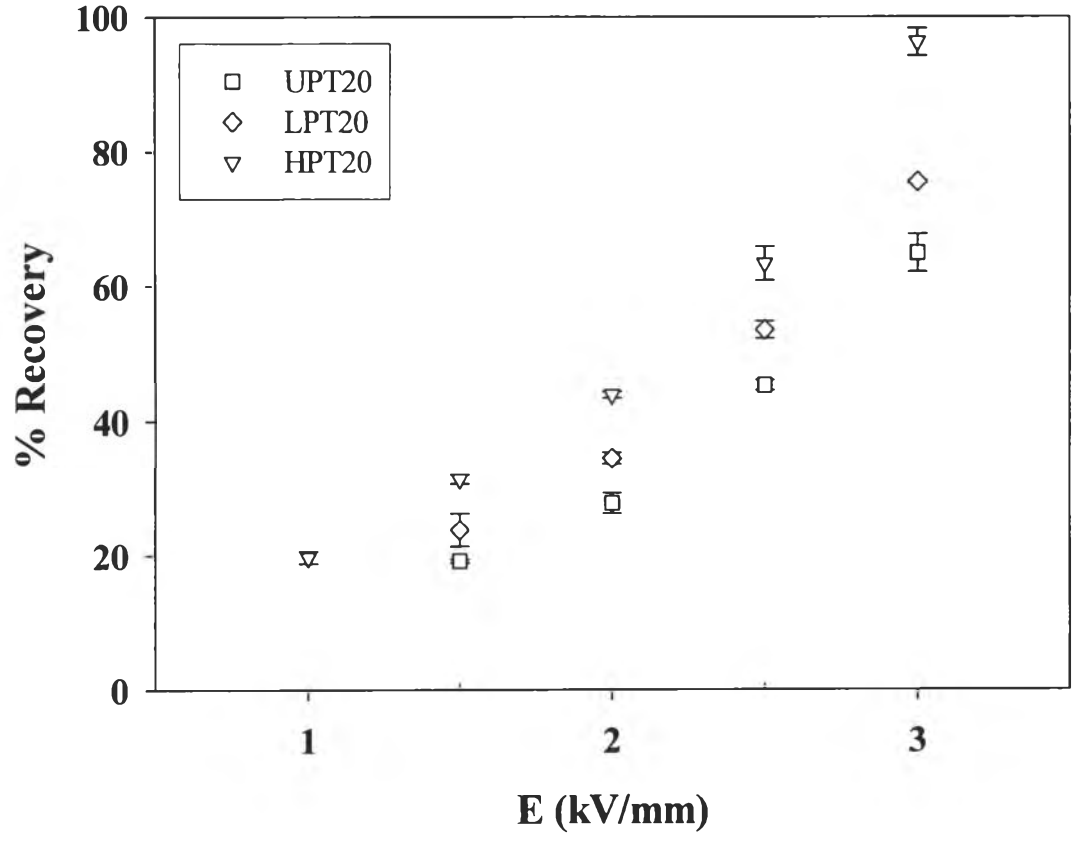

Figure 7.11 The % recovery as a function of the electric field strength of 20% wt. $HCLO_4$ doped PTAA suspensions at a constant applied shear stress of 50 Pa.